FOUR ROTOR POSITION AND SPEED SIMPLIFIED ESTIMATORS FOR VECTOR CONTROL OF HIGH-SPEED SPMSM, WITH TEST COMPARISONS

Răzvan ANCUȚI[*], Gheorghe-Daniel ANDREESCU[**], Ion BOLDEA[*]
[*]Dept. Electrical Machines and Drives, [**]Dept. Automation and Applied Informatics, University Politehnica of Timisoara,
Vasile Parvan Blvd., 2, 300223 Timisoara, Romania, Phone/Fax: +40-256-204402
Email: ancuti_r@yahoo.com, daniel.andreescu@aut.upt.ro, boldea@lselinux.upt.ro

Dorin ILES-KLUMPNER
ebm-papst St. Georgen GmbH & Co. KG, 78112, St. Georgen, Germany, Email: iles@ieee.org

Abstract: *The surface permanent magnet synchronous machines have a very simple structure due to the fact that L_d=L_q and thus they are favored for high-speed applications. The simplicity of these motors raises problems when sensorless control is desired for the reason that position and speed estimators do not behave, at low speeds, as well as they do in induction and interior permanent magnet synchronous machines. In high-speed applications the online computing cycle is small and therefore simplified position/ speed estimators are needed. Four rotor position and speed simplified estimators were implemented and compared to be used in encoderless systems. Several experimental drive tests are demonstrated, with experimental results showing the effectiveness of all implemented position and speed estimators, in high-speed range.*

Key words: *sensorless control, PMSM, high-speed control, position and speed estimator.*

1. Introduction

Asynchronous ac machines are the most widespread motors, known as being the workhorse in industrial drives, and large efforts are still made to improve their efficiency and to develop new kinds of motors for industrial applications [1]. A good alternative for this kind of applications are the surface permanent-magnet synchronous machines (SPMSM), which have many advantages such as high power density, torque to inertia ratio and energy efficiency [2], and make them attractive candidates for direct drive systems.

For a better control of synchronous machines with fast speed (torque) response, an encoder is necessary to be used. Controlled in this way, the synchronous motors can successfully replace the asynchronous motors and dc machines in various working conditions, maintaining in the same time the advantages presented above. The major encoder drawbacks are its relatively high cost and performance degradation due to vibration or humidity [3].

Another alternative is to outfit the machine with Hall sensors. Unfortunately, this method does not confer good dynamics because the Hall sensors give low resolution angle information that is not sufficient for complete operation range [4].

The most reasonable control of this kind of motors is without encoder. The first importance in this case is the way of rotor building. Thus from the control point of view, at low speeds, it matters if L_d is equal to L_q or not, so the motor design is very important when good operation at low speeds is desired [6].

Generally, in sensorless control of SPMSM (L_d=L_q), position and speed estimators based on emf begin to act properly only from speed values greater than 10% rated speed. The main drawback of these estimators is low and zero speed operation, where they fail since the back-emf information is too low [7]. They need also very well known parameters. Fortunately, in high-speed applications, self-starting over light load is frequently, and low-speed operation is scarce. Finally, limited on-line computing cycles are available in control of high-speed drives, so simplified, but reliable position/speed estimations are required. References [8] to [15] present different strategies of sensorless control for PMSMs, each with its merits and demerits.

In this paper, four position and speed estimators are presented. They can be used in control of ac machines, in particularity for SPMSM. For the case study here, we consider a high-speed SPMSM with the data shown in the Table 1 of Appendix.

2. Mathematical model of SPMSM

The SPMSM is generally assumed to have three balanced phases connected in Y or Δ configuration. The SPMSM model in stator coordinates is:

$$\overline{V}_s = R_s \bar{i}_s + \frac{d\overline{\lambda}_s}{dt}, \quad (1)$$

$$\overline{\lambda}_s = L_s \bar{i}_s + \overline{\lambda}_{PM}, \ \overline{\lambda}_{PM} = \lambda_{PM} e^{j\theta_r}, \ \bar{i}_s = i_s e^{j\theta_i} \quad (2)$$

where: $\overline{V}_s$, $\bar{i}_s$ and $\overline{\lambda}_s$ are the stator voltage, current and flux vectors, respectively, $\overline{\lambda}_{PM}$ is the PM-flux vector, R_s, L_s are the stator resistance and inductance, θ_r is the rotor position, and θ_i is the stator current vector angle.

The back-emf vector $\overline{E}$ is given by:

$$\overline{E} = \frac{d\overline{\lambda}_{PM}}{dt} = \omega_r \lambda_{PM} e^{j(\theta_r + \pi/2)}, \quad (3)$$

where ω_r is the rotor speed.

By inserting (2) in (1) and using (3):

$$\overline{E} = \overline{V}_s - R_s \bar{i}_s - L_s \frac{d\bar{i}_s}{dt}. \quad (4)$$

In steady state, the current vector speed $\omega_i = \omega_r$, and therefore by using (2), eq. (4) can be written as:

$$\overline{E} = \overline{V}_s - R_s \bar{i}_s - j\omega_r L_s \bar{i}_s. \quad (5)$$

Eqs. (1), (4) and (5) for SPMSM in stator reference frame will be used in position and speed estimators in the next chapter.

Fig. 1 shows the SPMSM space vector diagram.

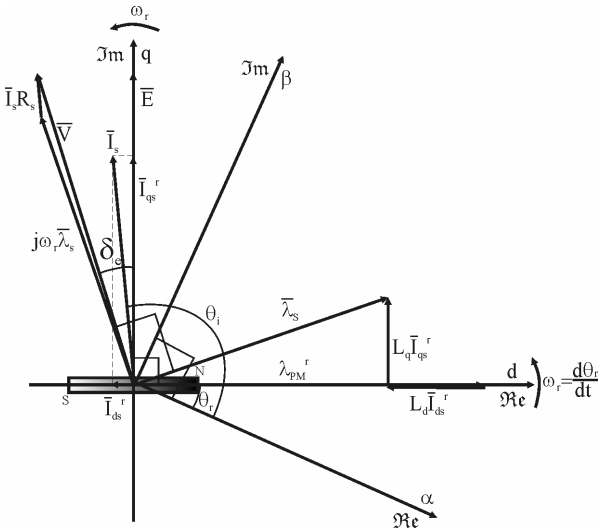

Fig. 1. Space vector diagram of SPMSM.

The SPMSM control structure (Fig. 3) uses speed control with position encoder, and employs standard current-vector control algorithm ($i_d^* = 0$) with two voltage-decoupling loops (6).

$$V_{dq\_ff}^* = -L_s \omega_r i_q^* + j\omega_r (\lambda_{PM} + L_s i_d^*). \quad (6)$$

3. Rotor position and speed estimators for encoderless control

The main feature of the proposed sensorless control techniques is that all of them use only current sensors. The input voltages (V_a, V_b, V_c) or (V_α, V_β) are replaced by the inverter reference voltages (V_a^*, V_b^*, V_c^*), respectively (V_α^*, V_β^*). Without voltage sensors, some approximations can be made for the back-emf. In fact this means to neglect voltage harmonics, delay of time response due to power switches commutations, and voltage drop on power switches. Four rather simple rotor position estimators suitable for high-speed applications are introduced below.

3.1. Permanent-magnet flux angle estimator

The PM-flux vector angle is identical with the rotor position θ_r. The estimator based on PM-flux vector $\overline{\lambda}_{PM}$ (Fig. 2) consists in 3 parts. The 1st part estimates the stator flux vector $\overline{\lambda}_s$ using the voltage model in stator reference frame (1) with a PI loop for dc offset compensation:

$$\overline{\lambda}_s = \int (\overline{V}_s - \bar{i}_s R_s - \overline{V}_{comp}) dt,$$
$$\overline{V}_{comp} = (k_p + \frac{k_i}{s}) \overline{\lambda}_s. \quad (7)$$

The 2nd part estimates $\overline{\lambda}_{PM}$ from (2):

$$\overline{\lambda}_{PM} = \overline{\lambda}_s - L_s \bar{i}_s. \quad (8)$$

The 3rd part gives the PM-flux module λ_{PM} and the rotor position by $\sin\theta_r$ and $\cos\theta_r$, which are directly used in rotation operators.

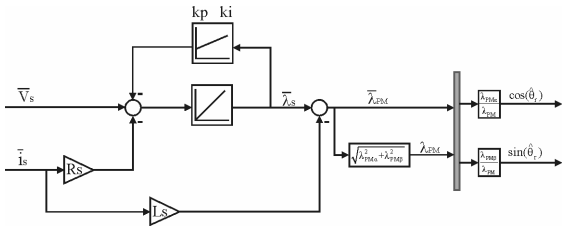

Fig. 2. Rotor position estimator based on PM-flux vector.

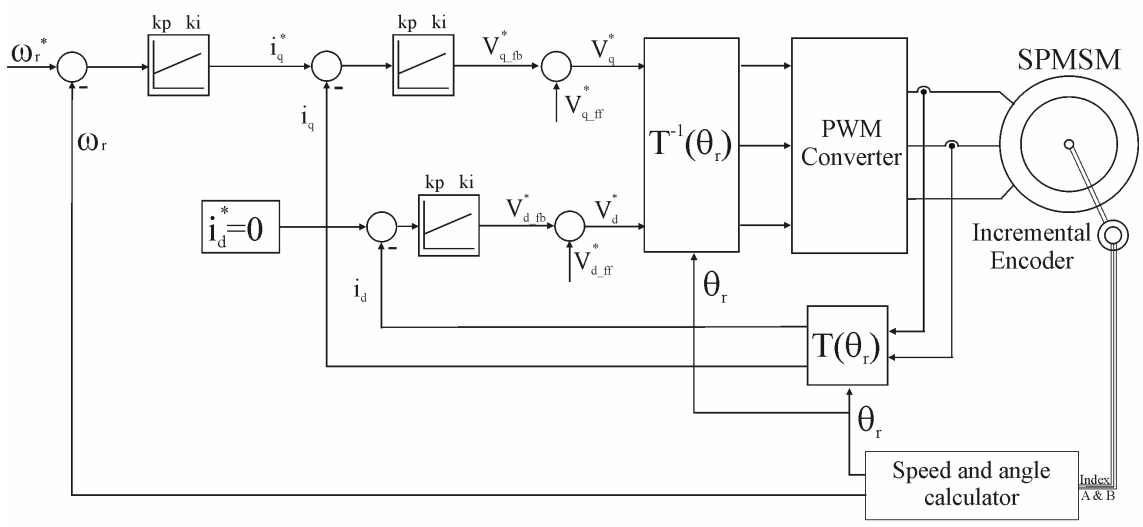

Fig. 3 Block diagram of vector control scheme with encoder position sensor.

3.2. Back-emf angle estimator in steady-state operating mode

The back-emf vector $\overline{E}$ is dephased exactly at $\pi/2$ from the *d* axis (3). The estimator from Fig. 3 is based on calculation of $\overline{E}$ in steady-state (5):

$$E_\alpha = V_\alpha - R_s i_\alpha + L_s \omega_r i_\beta, \qquad E_\beta = V_\beta - R_s i_\beta - L_s \omega_r i_\alpha. \tag{9}$$

A phase-locked loop (PLL) state-estimator extracts the rotor position and speed from $\overline{E}$ vector.

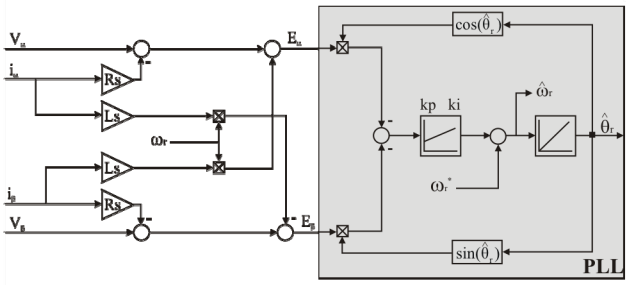

Fig. 4. Rotor position and speed estimator based on back-emf in steady-state operating mode.

3.3. Back-emf angle estimator for dynamic operating mode

The estimator-version from Fig. 5 is closed up to Fig. 4, but the back-emf vector $\overline{E}$ is calculated from (4). It is valid for transients and has the components:

$$E_\alpha = V_\alpha - R_s i_\alpha - L_s di_\alpha / dt, \qquad E_\beta = V_\beta - R_s i_\beta - L_s di_\beta / dt. \tag{10}$$

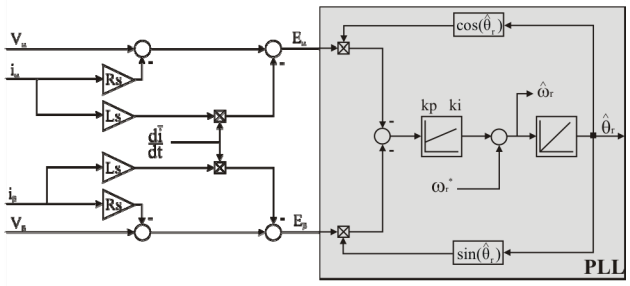

Fig. 5. Rotor position and speed estimator based on back-emf in dynamic operating mode.

To reduce noises in current derivatives di_s/dt, a filter-based derivative estimator (Fig. 6) is used [11].

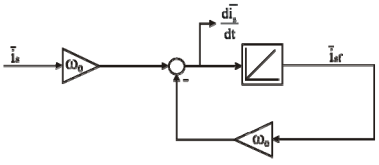

Fig. 6. Derivative estimator based on filter technique.

3.4. Voltage-based angle estimator

This type of estimator uses the voltage vector represented in two references: stator and rotor reference frames (see Fig. 1). Thus, in each moment, if both (V_α, V_β) and (V_d, V_q) computed voltages at the previously sampling period are known, the voltage angles to the axis α, respectively, axis *d* can be estimated as:

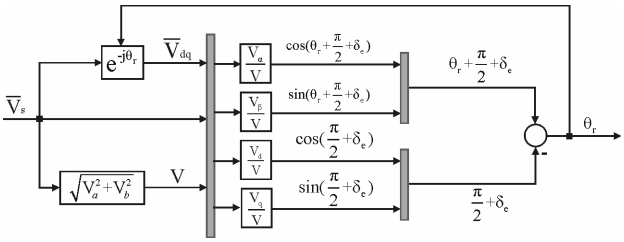

Fig. 7. Voltage angle calculation related to α and d axes.

$$V_d = V_\alpha \cos\theta_r - V_\beta \sin\theta_r$$
$$V_q = V_\alpha \sin\theta_r + V_\beta \cos\theta_r, \quad (11)$$

$$\theta_r = (\theta_r + \pi/2 + \delta) - (\pi/2 + \delta). \quad (12)$$

Computing the difference between the two angles in (12), the rotor position can be estimated. The implementation of this estimator is shown in Fig. 7.

The implementation of the position and speed estimator can be also made in the way presented in [7] and [8]. It is shown (see Fig. 3) that the output of the current regulator $V^*_{d\_fb}$ has unexpectedly bad results. Even more, the drawback of this method is that it employs, together with vector control or another control method, the transformation $\alpha\beta \to dq$ that requires rotor position θ_r. Note that for the estimators presented above, the estimators 1 to 3 do not use rotation operators, while the estimator 4 uses it.

4. Rotor speed estimator for encoderless control

The rotor speed ω_r can be estimated from the rotor position θ_r. All estimators previously presented estimate rather well rotor position. The estimators 2 and 3 contain the speed estimation, which can be used efficiently in control. For the estimators 1 or 4 that give rotor position estimation, a phase-locked loop (PLL) speed estimator was introduced as in Fig. 8.

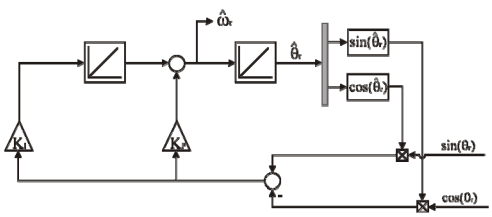

Fig. 8. Speed estimator based on rotor position given by the estimators 1 or 4.

The gains k_p and k_i could be computed, for example, using the pole placement method. Thus, if the system poles are p_1 and p_2 then:

$$k_p = -(p_1 + p_2), \quad k_i = p_1 p_2. \quad (13)$$

This method is an analytical one, but a trial and error method can also be applied [10] with good results, even if the system is very complex and computation delays should be taken into account.

5. Test platform description

The SPMSM drive system for the laboratory prototype tests is illustrated in Fig. 9. Two identical 0.8 kW, 20,000 rpm, four pole SPMSMs with sinusoidal back-emf are mechanically coupled (Fig. 10). The data for these motors are presented in Table 1 in Appendix. The motor is serial connected with inductances per phases (L_f), and it is fed by a 42 V/ 300 A MOSFET inverter with a switching frequency of 20 kHz. The encoder has 500-pulse-per-revolution (ppr) and provides the real rotor position and speed.

All control algorithms were developed in Matlab-Simulink and implemented in DSpace 1103. The estimator coefficients, chosen with Ziegler Nichols method [10] were improved by a trial and error method and are specified in Table 2 of Appendix.

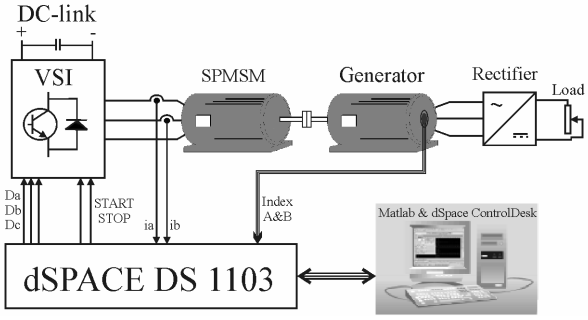

Fig. 9. Experimental system setup.

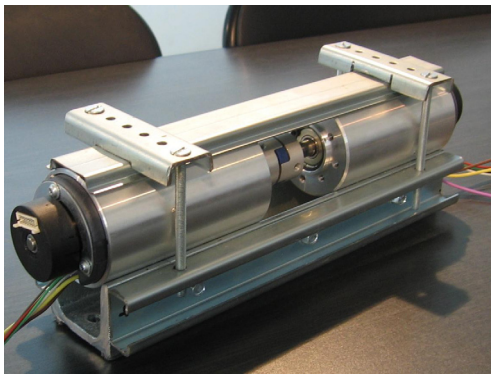

Fig. 10. Twin high-speed SPMSMs system.

6. Experimental results

All the described estimators were tested under encoder control. For a good image of estimators work, two tests considered very relevant have been performed: i) speed reversal from -10,000 rpm to +10,000 rpm, without load, and ii) 50% step rated-load perturbation torque at 10,000 rpm.

For the first test, the reference and the actual speeds are presented in Fig. 11.

Fig. 12 illustrates the speed error [%] of all 4 estimators in comparison with the speed feedback computed from encoder. Notable errors for estimator 1 and small errors for estimators 2 and 3 are visible at very low speed. The worst case is for the estimator 4. Fig. 13 shows the actual current for the speed reversal from -10,000 to 10,000 rpm.

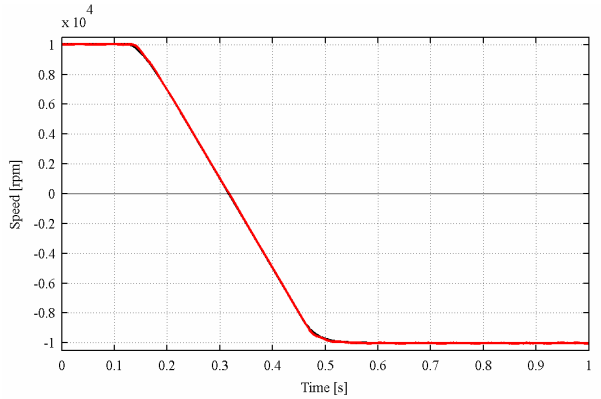

Fig. 11. Reference (thick line) and actual speed for speed reversal ±10,000 rpm, no loaded under encoder control.

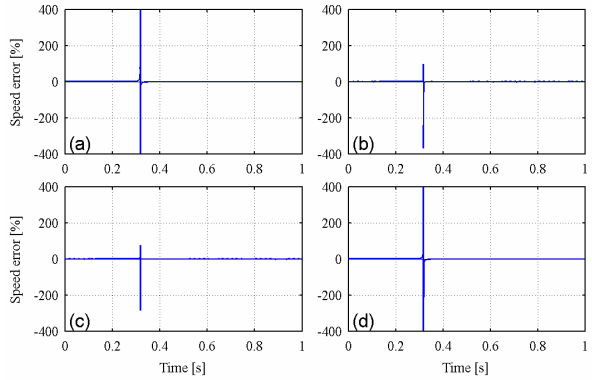

Fig. 12. Speed estimation versus encoder errors for estimators: 1(a), 2(b), 3(c), 4(d) for ±10 krpm, no loaded.

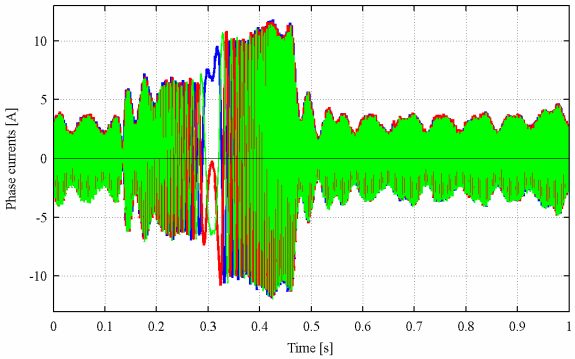

Fig. 13. Actual currents for speed reversal.

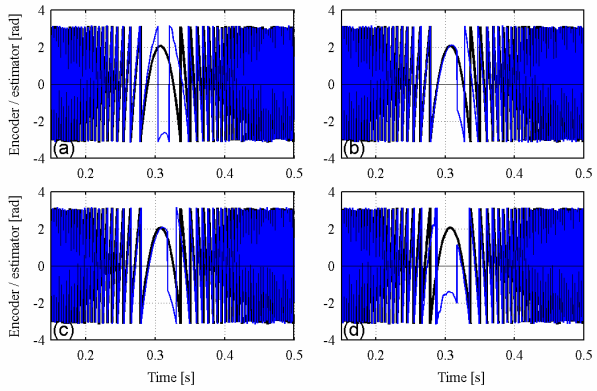

Fig. 14. Position estimation versus encoder (thick line) for 1(a), 2(b), 3(c), 4(d), for ±10 krpm, no loaded.

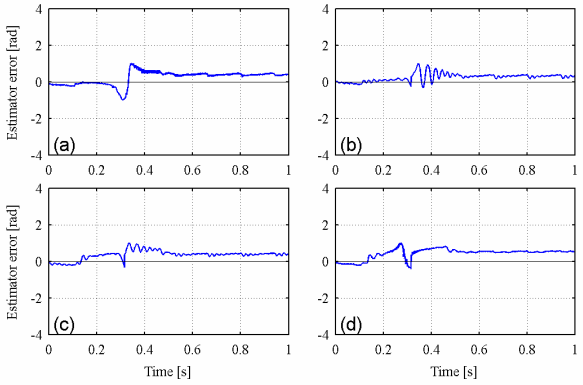

Fig. 15. Electric angle error between encoder and estimator: 1(a), 2(b), 3(c), 4(d), for ±10 krpm, no loaded.

The rotor position response of all estimators, in speed reversal during transient interval [0.15-0.5] s, is shown in Fig. 14. As can be seen, all estimators follow very closely the actual encoder position. Nevertheless, the absolute error could not be observed here, except for around zero speed.

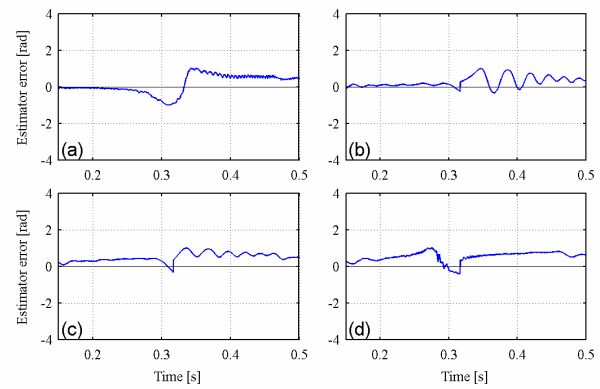

Fig. 16. Zoom of electric angle error between encoder and estimators: 1(a), 2(b), 3(c), 4(d), ±10 krpm, no loaded.

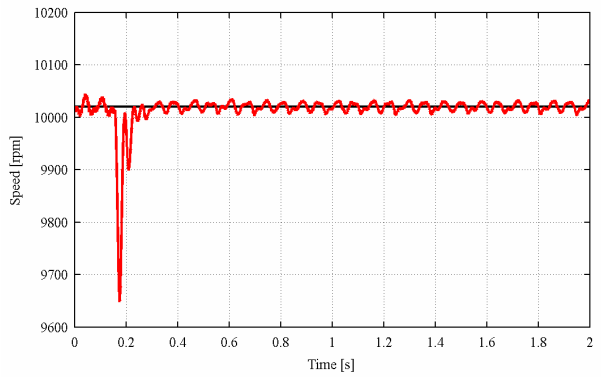

Fig. 17. Speed responses for 50% torque perturbation.

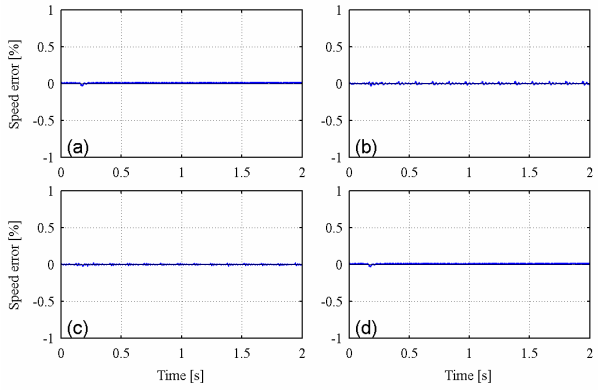

Fig. 18. Estimated speed versus encoder errors for estimators: 1(a), 2(b), 3(c), 4(d), at 10 krpm with 50% load torque perturbation.

For more clarity the position error for all 4 position estimators is given separately in Fig. 15 and in Fig. 16, during no load speed reversal ± 10,000 rpm reversal tests. All estimator errors are within 1 electrical radian. Only estimator 2 shows a zero average (steady state) error, though oscillatory Fig. 16 (b).

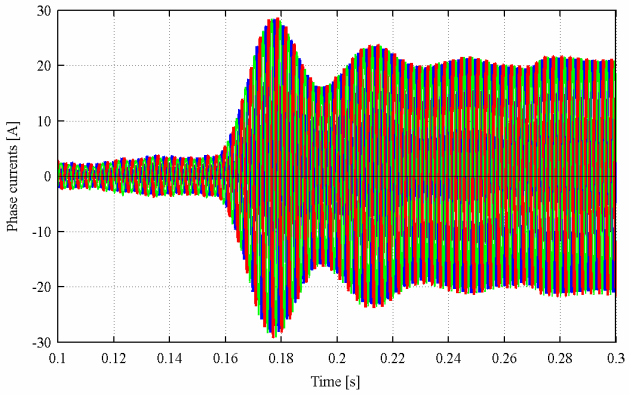

Fig. 19. Stator currents for 50% torque perturbation

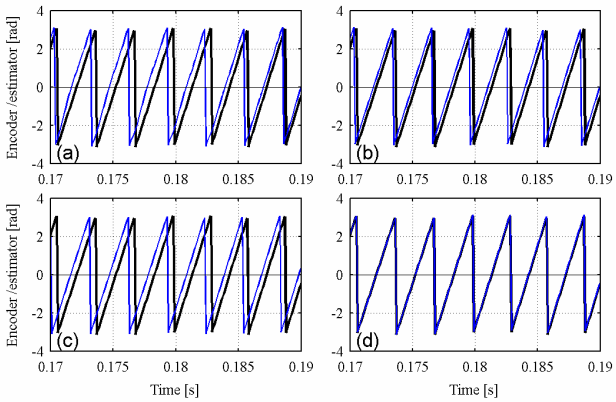

Fig. 20. Zoom of position estimation versus encoder (thick line) for 1(a), 2(b), 3(c), 4(d), at 10 krpm with 50% load torque perturbation.

The speed response to 50% step rated-load torque applied at 0.2 s at 10,000 rpm is presented in Fig. 17. It can be observed that in about 0.1 s the regulators bring the speed back to 10,000 rpm. During this heavy load transient, the speed error of all 4 estimators (Fig. 18) is within 1%

During the transients in Fig. 17, the actual motor currents are presented in Fig. 19 for a zoom region, where the event when the motor is loaded can be obviously seen. In Fig. 20 a zoom is represented when the estimators react differently (see Fig. 22). Fig. 21 and Fig. 22 show a comparison between the errors of the position estimated by all discussed estimators and the real position given by encoder at 10,000 rpm, with 50% load torque perturbation. It is evident that small errors of estimators are maintained even during step torque perturbations.

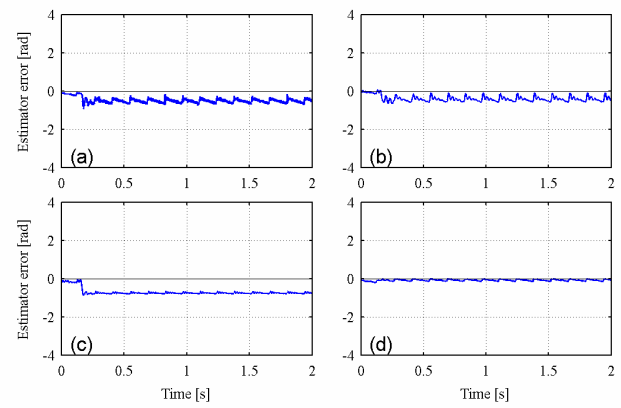

Fig. 21. Angle error between encoder and estimators: 1(a), 2(b), 3(c), 4(d), at 10 krpm with 50% load torque perturbation.

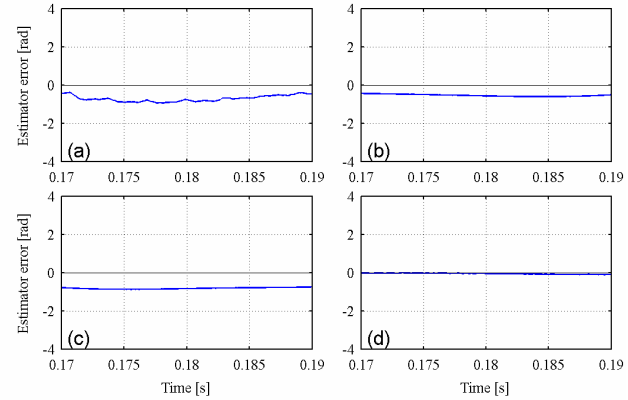

Fig. 22. Zoom of angle error between encoder and estimators: 1(a), 2(b), 3(c), 4(d), at 10 krpm with 50% load torque perturbation.

The best behavior belongs from estimator 3 (Fig. 21c) because there are no high-frequency oscillations which would harm sensorless high-speed control.

7. Conclusion

In the same operating conditions, four rotor position and speed estimators for surface mounted synchronous permanent magnet motors (SPMSMs) were tested. All of them operate for acceptable parameter values and have small errors. For high-speed encoderless system, a rotor position estimator with small oscillations should be used in implementation. In encoderless systems, the duration of position angle computation is decisive. If the estimated angle has big oscillations comparatively with the encoder angle, then the system will not operate properly. This is visibly at high-speed motors, where the angle estimator should be very fast and without big oscillations. In this case, the estimators 2 and 3 should be selected.

All rotor position and speed estimators have problems at low and especially zero speed. So, in sensorless control, an addition starting control strategy is required.

Appendix

Table 1. SPMSM specifications

Number of pole pairs (p)	2
Rated speed	20,000 rpm
Rated frequency	667 Hz
Rated torque	0.4 Nm (at 20,000 rpm)
Rated phase to phase voltage	39 V(rms)
Rated phase current	29.5 A(rms) (at 20,000 rpm)
Stator resistance per phase (R_s)	0.083 Ω
Inductance (L_s)	0.0425 mH
Serial inductance per phase (L_f)	0.15 mH
Rotor permanent-magnet (λ_{PM})	0.00635 V s rad^{-1}
Inertia of rotating system (J)	40*10^{-6} kgm^2
Viscous friction coefficient (B_m)	10^{-6}Nms/rad

Table 2. Gains used in real control system for PI controller: $k_p(1+k_i/s)$.

PI speed control Fig. 3	k_p	20
	k_i	0.06
PI current controllers Fig. 3	k_{p_dq}	1
	k_{i_dq}	6000
PLL Fig. 4 & Fig. 5	k_p	3
	k_i	7000
Derivative estimator Fig. 6	ω_0	1000
Speed estimator, Fig. 8	k_p	70
	k_i	1000

Acknowledge

This work was partially supported by the Romanian National University Research Council (CNCSIS) within the national grant of excellence CEEX no. X2C33/ 2006.

References

1. Montesinos, D, Galceran, S., Sudria, A., Gomis, O., Blaabjerg, F.: *Low cost Sensorless Control of Permanent Magnet Motors - An Overview and Evaluation*. In: Proc. IEEE Int. Conf. on Electric Machines and Drives, IEMDC 2005, San Antonio, TX, May 2005, pp. 1681-1688.

2. Chi, S., Xu, L., Zhang, Z.: *Sliding Mode Sensorless Control of PM Synchronous Motor for Direct-Driven Washing Machines*. In: Conf. Record of IEEE-IAS 2006, Tampa, FL, Vol. 2, Oct. 2006, pp. 873-879.
3. Kim, J.-S., Sul, S.-K.: *New Approach for High-Performance PMSM Drives without Rotational Position Sensors*. In: IEEE Trans. on Power Electronics, Vol. 12, No. 5, Sept. 1997, pp. 904-911.
4. Urlep, E., Horvat, J., Jezernik, K.: *Pseudo Sensorless Control of PMSM*. In: Proc. 12th Int. Power Electronics and Motion Control Conf., EPE-PEMC 2006, Portoroz, Aug. 2006, pp. 1950-1955.
5. Bumby, J.R., et al: *Electrical machines for Use in Electrically Assisted Turbochargers*. In: Proc. 2nd Int. Conf. on Power Electronics Machines and Drives, PEMD 2004, Vol. 1, March 2004, pp. 344-349.
6. Bianchi, N., Bolognani, S.: *Influence of Rotor Geometry of an Interior PM Motor on Sensorless Control Feasibility*. In: Conf. Record of IEEE-IAS 2005, Hong Kong, Vol. 4, Oct. 2005, pp. 2553-2560.
7. Seok, J.-K., Lee, J.-K.. Lee, D.-C.: *Sensorless Speed Control of Nonsalient Permanent-Magnet Synchronous Motor Using Rotor-Position-Tracking PI Controller*. In: IEEE Trans. on Industrial Electronics, Vol. 53, No. 2, April 2006, pp. 399-405.
8. Bae, B.-H., Sul, S.-K., Kwon, J.-H., Byeon, J.-S.: *Implementation of Sensorless Vector Control for Super-High-Speed PMSM of turbo-compressor*. In: IEEE Trans. on Industry Applications, Vol. 39, No. 3, May-June 2003, pp. 811-818.
9. Lorenz, R.D., Van Patten, K.W.: *High-Resolution Velocity Estimation for All-Digital, AC Servodrives*. In: IEEE Trans. on Industry Applications, Vol. 27, No. 4, July-Aug. 1991, pp. 701-705.
10. Ziegler, J.G., Nichols, N.B.: *Optimum Settings for Automatic Controllers*. In: Trans. of American Society of Mechanical Engineers (ASME), Vol. 64, Nov. 1942, pp. 759-765.
11. Andreescu G.D.: *Estimatoare în sisteme de conducere a acționărilor electrice - Aplicații la MSMP (Estimators in Control of Electric Drives -Applications to MSMP)*, Editura Orizonturi Universitare, Timişoara, 1999.
12. Ostlund, S., Brokemper, M.: *Sensorless Rotor-Position Detection from Zero to Rated Speed for an Integrated PM Synchronous Motor Drive*, In: IEEE Trans. on Industry Applications, Vol. 32, No. 5, Sept.-Oct. 1996, pp. 1158-1165.
13. Chung, D.-W., Kang, J.-K., Sul, S.-K.: *Initial Rotor Position Detection of PMSM at Standstill without Rotational Transducer*. In Int. Conf. Electric Machines and Drives, IEMD'99, Seattle, WA, May 1999, pp. 785-787.
14. Nakashima, S., Inagaki, Y., Miki, I.: *Sensorless Initial Rotor Position Estimation of Surface Permanent-Magnet Synchronous Motor*. In: IEEE Trans. on Industry Applications, Vol. 36, No. 6, Nov.-Dec. 2000, pp. 1598-1603.
15. Silva, C., Asher, G.M., Sumner, M.: *Hybrid Rotor Position Observer for Wide Speed-Range Sensorless PM Motor Drives Including Zero Speed*. In: IEEE Trans. on Industrial Electronics, Vol. 53, No. 2, April 2006, pp. 373-378.